JOURNAL OF AIRCRAFT
Vol. 30, No. 5, Sept.–Oct. 1993

Lateral Aerodynamic Interference Between Tanker and Receiver in Air-to-Air Refueling

A. W. Bloy,* M. G. West,† K. A. Lea,‡ and M. Jouma'a‡
University of Manchester, England, United Kingdom

Wind-tunnel data have been obtained from a tapered tanker wing and receiver aircraft model at varying vertical separation. The data are presented in derivative form and compared with theory using a flat vortex sheet model of the tanker wing wake to determine the induced angle-of-attack variation on the receiver wing, fin, and tailplane due to the tanker wing. Aerodynamic loads on the receiver are obtained by the vortex lattice method, with an allowance made for the vertical displacement of the tanker wake in the estimation of the fin side force. In the experiments, the lateral aerodynamic interference between tanker and receiver was determined by banking the tanker wing and displacing it sideways, and by yawing the receiver aircraft model. Data were obtained from open and closed test sections in order to assess the significant boundary interference effect and corrections estimated from the image vortex system of the tanker and receiver wings in the test section. In general, the theory compares favorably with the experimental data. The most significant terms are the rolling moments due to sideways and bank displacements. Significant side forces are produced due to sidewash on the fin from the tanker and receiver wings and, when displaced in yaw, the receiver experienced a loss in directional stability.

Nomenclature

b = wing span
C_L = lift coefficient, $L/q_\infty S$
C_l = rolling moment coefficient, $L/q_\infty Sb$
C_n = yawing moment coefficient, $N/q_\infty Sb$
C_Y = side force coefficient, $Y/q_\infty S$
L = lift
L = rolling moment
N = yawing moment
$Oxyz$ = axes fixed in aircraft with origin at center of gravity and inverted with model in wind tunnel
q = dynamic pressure
S = wing area
s = wing semispan
V = airspeed
v = velocity component along Oy
w = velocity component along Oz
x = horizontal displacement from quarter chord point of the tanker wing, positive in the forward direction in the plane of symmetry
Y = side force
y = sideways displacement from the plane of symmetry of the tanker wing, positive to starboard
z = vertical displacement of the quarter chord point of the receiver wing from the quarter chord point of the tanker wing
α = angle of attack
β = sideslip angle
Γ = circulation
ϕ = bank angle
ψ = yaw angle

Subscripts
R = receiver aircraft
T = tanker wing
w = wake of tanker aircraft
∞ = free flight conditions

Received March 27, 1992; revision received July 13, 1992; accepted for publication July 13, 1992.

*Lecturer in Engineering (Aero), Department of Engineering.
†Research Assistant, Department of Engineering.
‡Research Student, Department of Engineering.

Introduction

BRADLEY[1] has described a typical refueling maneuver for large receiver aircraft using the probe and drogue method for air-to-air refueling. The receiver aircraft joins with the tanker in the echelon position with the tanker fuel hose fully trailed to a length of 25 m. The receiver moves from the echelon position to a position 15–30 m astern of and below the drogue, and advances up the line of the hose at an overtaking speed of 1.5–2 m/s. At a position 3–4.5 m behind the drogue, the receiver is held in a stabilized "precontact" position. A small power increment is applied to re-establish the overtaking speed and the probe is flown into contact with the drogue. The receiver continues to close on the tanker until about 12–15 m of hose remains extended, giving a safe separation of about one wing span or less. From flight tests on large receiver aircraft carried out at the Aeroplane and Armament Experimental Establishment, Bradley concluded that all the aircraft types tested have the potential to be air-to-air refueling receivers from various tankers, although handling problems were experienced by some receiver aircraft at various points in the flight envelope.

In previous papers on air-to-air refueling by Bloy et al.[2–4] the aerodynamic interference between particular tanker and receiver aircraft was modeled and its effect on the performance, stability, and control of the receiver analyzed. Horizontal separation distances of 1.5–2 wing spans were considered and a simple horseshoe vortex was used to model the tanker wake. The loads on the receiver due to the tanker downwash and sidewash were estimated using several methods including the method developed by Kuchemann[5] for swept wings, and the vortex-lattice method programed by Margason and Lamar.[6]

Wind-tunnel tests were then made by Bloy et al.[7,8] in order to obtain data on the aerodynamic interference between the tanker and receiver for comparison with theory. Similar rectangular wings of aspect ratio 5 with and without flaps were used to represent the tanker wing. This wing was supported on a traverse which allowed bank, pitch, spanwise, and vertical displacements relative to a receiver aircraft model which consisted of a main wing identical to the tanker wing together with a rectangular fin and tailplane. A horizontal separation

between the tanker wing and receiver aircraft model of less than one wing span was used. In the case of the flapped tanker wing, the wake was represented by a pair of horseshoe vortices from both the wing and flap tips. Either lifting-line theory or the vortex-lattice method were used to estimate the loads on the receiver aircraft model. For the flapped tanker wing, data were obtained from open and closed test sections in order to estimate the wind-tunnel boundary interference effect. Large differences were found between theory and experiment due mainly to the boundary interference and incomplete roll up of the trailing vortices. The latter effect was demonstrated by comparing the experimental data with the theoretical results obtained from both horseshoe vortex and plain vortex sheet models of the tanker wing wake. The differences were greatest for the rolling moment due to sideways displacement, which is the most significant lateral aerodynamic interference term. In this case, the data lie between the theoretical results from the horseshoe vortex model, which overpredicts, and the plain vortex sheet model. However, the overall theoretical and experimental trends are similar.

This article presents results for a more realistic tapered tanker wing which was tested with the receiver aircraft model and at the wind-tunnel conditions used previously by Bloy et al.[7,8] Since more vorticity is shed inboard on a tapered wing, the trailing vortex roll up takes place more slowly compared with a rectangular wing of the same aspect ratio. Grow[9] has presented measurements which show that only a small fraction of the vortex sheet from a highly tapered wing, similar to the tanker wing model described in this article, is rolled up at a distance of approximately one wing span downstream. Extensive flowfield surveys of the wake behind two swept wings of taper ratio 1/3 (= tip chord/root chord) were carried out by El-Ramly and Rainbird.[10] It was found that at 5–10 wing spans downstream, less than 60% of the wing root circulation had rolled up into the core of the tip vortex, and at 1.7 chords downstream of the wing trailing edge, the tip vortex contained only one third of the circulation at the wing root.

Other work related to the aerodynamic interference between tanker and receiver aircraft during air-to-air refueling is extremely limited. Hoganson[11] evaluated the longitudinal aerodynamic interference between the KC10 tanker and a B52 receiver. At the contact position the horizontal separation was 38 m or 0.76 times the tanker wing span. The rolling-up process of the tanker's wing tip vortices was not considered, the tanker wake being represented by a flat vortex sheet, and the vortex-lattice method was used to evaluate the interference effects.

Experimental Setup

The experiments were performed in the subsonic wind tunnel at the Goldstein Aeronautical Engineering Research Laboratory of the University of Manchester using an experimental arrangement similar to that described in previous work.[7,8] The test section is 0.87 by 1.13 m. An unswept, straight tapered wing of taper ratio 0.244 and identical in span to the rectangular wing tested previously was used to represent the tanker. This wing was supported in the open test section at each wing tip by a tapered horizontal bar fixed to a traverse which allowed bank, pitch, spanwise, and vertical displacements of the wing, while the receiver aircraft model was able to yaw on the wind-tunnel balance. For the closed test section experiments, a simpler tanker wing support system with vertical struts was used. This system did not allow any bank movement. The receiver aircraft model consisted of a main rectangular wing with the same span as the tanker wing, and a rectangular tailplane and fin attached to a center boom from the wing. This model was used in the previous experiments[7,8] and tests were performed at a horizontal separation, measured between the quarter-chord points of the tanker and receiver wings, of 0.55 m or 0.72 times the wing span. This separation is close to that used in contact between the tanker and receiver aircraft during air-to-air refueling. Some yaw tests were repeated in the open test section with the tanker wing attached to a circular fuselage. The wing was set low and at an incidence of 4 deg on the fuselage. Relevant dimensions of the models and the positions within the test section are given in Fig. 1. For the receiver aircraft model, all airfoil sections were NACA 0015 sections, and the tailplane was set level with the wing at the lowest position on the fin. The tanker wing used the NACA 0018 section.

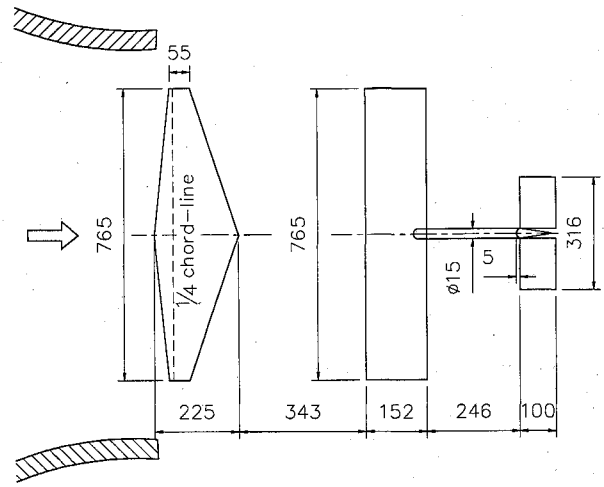

Fig. 1 Dimensions of tanker wing and receiver aircraft model and position in wind-tunnel test section.

For the tests, the receiver aircraft model was mounted inverted on a six-component balance linked to a data acquisition system and positioned 0.15 m above the centerline of the wind tunnel. The tanker wing was traversed vertically varying the vertical separation between tanker and receiver from 0.05 to 0.2 m or 0.3 m. As reported in Ref. 8, the corrections due to the wind-tunnel boundary interference were significant due to the relatively high ratio of the wing span to tunnel span of 0.7. In order to assess the magnitude of the wind-tunnel boundary interference, measurements were taken in both open and closed test sections. The interference is extremely large when the tanker wing is displaced sideways towards the tunnel wall and an estimate of the interference effect was made using the image vortex system for the tanker and receiver wings in a rectangular test section. The method assumes horizontal tanker and receiver wing wakes and involves estimation of the induced angle of attack variations on both the tanker and receiver wings due to the image vortex system. The effective twist distributions are then included in the theoretical model of the tanker and receiver wing combination. The greatest effect is on the receiver rolling moment derivative $\partial C_{l_R}/\partial(y_T/b)$, and the corresponding experimental data are presented in both corrected and uncorrected form.

Aerodynamic Model

As discussed in the introduction, the flat vortex sheet model of the tanker wing wake appears to be more applicable to the tapered wing than the horseshoe vortex model used previously for the rectangular wing. Therefore, the vortex-lattice method of Margason and Lamar[6] was applied to the tanker wing using 30 spanwise and 4 chordwise points across the wing. This number of points was found to be sufficiently accurate. The wing incidence was chosen so that the measured lift matched that obtained previously using the rectangular wing at the same wind-tunnel airspeed of 37 m/s. This resulted in a lift coefficient of 0.544. The corresponding theoretical spanwise lift distribution is shown in Fig. 2, whereas, downwash distributions at the position of the receiver main wing and sidewash distributions at the position of the receiver fin are shown in Fig. 3. However, the vortex-lattice method does not produce the correct sidewash close to the vortex sheet given by $v_w = \pm\frac{1}{2}(d\Gamma/dy)$, since the sidewash is either zero or infinite,

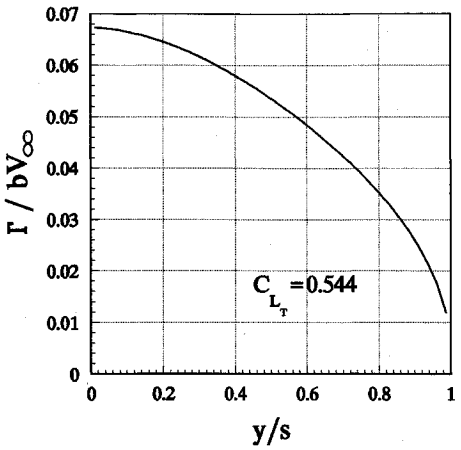

Fig. 2 Spanwise distribution of circulation on tanker wing.

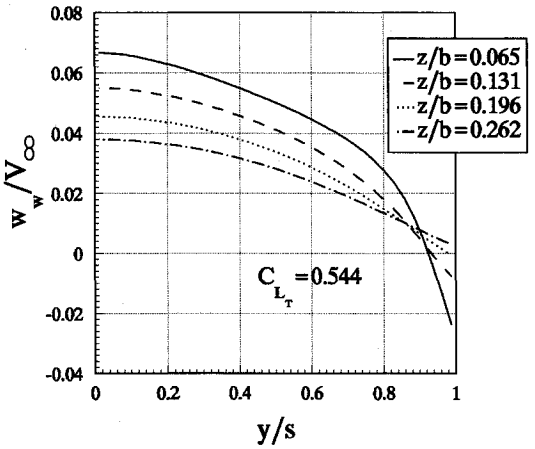

Fig. 3a Downwash induced by tanker wing at position of receiver main wing.

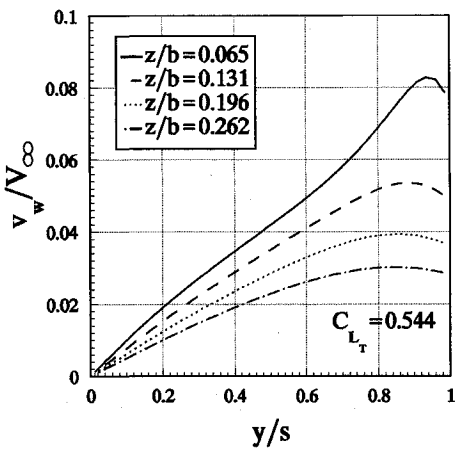

Fig. 3b Sidewash induced by tanker wing at position of receiver fin.

depending on whether the point of interest lies between or on the trailing vortices. Alford[12] obtained more realistic values of the sidewash velocity close to the vortex sheet by estimating the sidewash in the plane of the wing due to the lateral gradient of the circulation and fairing from this value to the maximum sidewash obtained by the vortex lattice method slightly below the wing. In this article the receiver main wing and tailplane are analyzed at positions below the tanker wing vortex sheet, although the fin intersects the vortex sheet at low values of the vertical separation z/b between tanker and receiver. It was found, however, that the region in which the sidewash is incorrect is relatively small and has a negligible effect on the fin side force.

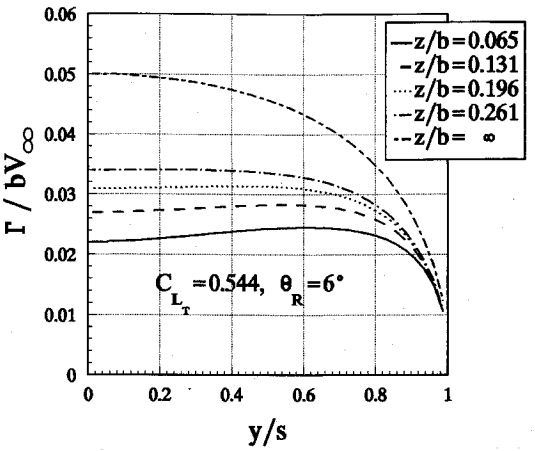

Fig. 4 Spanwise distribution of circulation on receiver wing.

As in the previous work,[7,8] the loads on the receiver aircraft model were estimated by determining the induced flow velocity normal to the receiver wing, tailplane, or fin, due to the tanker wake. The effect of the induced normal flow component is then assumed to be identical to that of an appropriately twisted wing in uniform flow. The vortex lattice method was used to determine the aerodynamic loads on the receiver wing, tailplane, and fin. Typically, 30 spanwise and 4 chordwise points were used on the fin and each half of the tailplane. Upstream influence of the receiver aircraft wing on the tanker wing was neglected since the estimated change in the tanker wing angle of attack due to the receiver is $1\frac{1}{2}\%$. For the receiver wing and tailplane, the induced rolling and yawing moments depend mainly on the asymmetric distribution of the downwash over the wing and tailplane as the receiver is displaced from the zero sideslip, wings level position on the centerline of the tanker wake, although the contribution due to the tailplane, which is in the downwash of both the tanker and receiver, is relatively small. In the case of the fin, the side load is due mainly to the tanker sidewash and the component of downwash acting normal to the fin following a displacement in bank angle. This load was estimated using the vortex-lattice method applied to the fin and low tailplane combination and allows for the interference between the two surfaces. As a first approximation, the vertical displacement at the center of the tanker wake has been estimated by integrating the downwash angle downstream from the trailing edge of the tanker wing, and this wake displacement has been taken into account in the estimation of the forces on the fin and tailplane. The wing rolling and yawing moments, however, depend mainly on the changes in lift and induced drag near the wing tips, and in this region the displacement of the vortex wake is small and has been neglected in the estimation of the wing moments. A more precise analysis obviously requires a model of the vortex sheet roll up.

Due to the downwash from the tanker, the lift distribution on the receiver is significantly modified with more lift produced outboard and less inboard, as shown in Fig. 4. When the receiver is displaced, particularly in the yaw case, there is a significant sidewash at the receiver fin due to the receiver main wing. When the fin lies below the tanker vortex wake, this effect enhances the sidewash due to the tanker. In order to estimate this sidewash component, a flat vortex sheet model of the receiver main wing wake was used with an allowance for the vertical displacement at the center of the wake. As described in a previous paper,[7] a consequence of banking the tanker wing in the experiment, rather than the receiver aircraft model, is that the receiver experiences both bank and sideways displacements relative to the center line of the tanker wing vortex wake.

Experimental Results and Comparison with Theory

Initially, the tapered tanker wing was supported on the wind-tunnel balance and tested to obtain its lift characteristics

in both the open and closed test sections. The experimental data, together with the theoretical lift slope obtained using the vortex-lattice method, are shown in Fig. 5. The wind-tunnel boundary interference effect produces 15% difference between the closed and open test section data. In the subsequent experiments on the aerodynamic interference between the tanker wing and receiver aircraft model, the tanker wing was set in the open and closed test sections at a lift coefficient of 0.544. The tunnel airspeed for all of the tests was 37 m/s giving a Reynolds number based on the wing chord of 3.8×10^5.

Lateral tests were performed in the open test section by displacing the tanker wing sideways and in bank on its support frame, and by rotating the receiver aircraft model in yaw on the wind-tunnel balance. According to the usual convention, sideways displacement is taken as positive with the tanker wing moving to the starboard side. Positive bank displacement corresponds to the starboard wing moving up since the tanker wing is inverted in the wind tunnel. Banking the tanker wing rotates the wing wake and effectively moves the receiver aircraft model by a relatively small amount to starboard. The effect of positive bank and side displacements is to increase the downwash on the starboard wing of the receiver and reduce the downwash on the port wing. The resulting rolling moment terms, due to sideways and bank displacements, are then positive. The side force and yawing moment on the receiver are mainly due to the sidewash at the fin following a sideways or yaw displacement, and the component of downwash normal to the fin following a bank displacement. Both positive bank and side displacements produce a side force on the fin which acts towards the port side with an associated yawing moment in the positive direction. In the yawing case, positive yaw of the receiver rotates the nose of the receiver to starboard, inducing negative sideslip in the wind tunnel and displacing the fin to the port side. The sidewash from the tanker wing and receiver wing wakes then induces a side force on the fin to port and a positive destabilizing yawing moment. For the closed test section experiments, a simpler tanker wing support system which did not allow any bank movement was used. In all of the lateral tests, the receiver aircraft model was tested at 6-deg pitch angle to the horizontal.

From the experimental results it was observed that the variations of the aerodynamic side force, rolling, and yawing moments with sideways, bank, and yaw displacements are essentially linear within experimental accuracy and over the range of displacements tested. This allows the aerodynamic data to be presented in derivative form. Similar, essentially linear, variations were obtained from the theory as shown in Fig. 6 which gives the typical variation of the rolling moment on the receiver aircraft due to sideways displacement of the tanker wing. The direction of the rolling moment is in the stable sense, since the receiver aircraft would roll so that the sideways component of the receiver aircraft lift vector tends

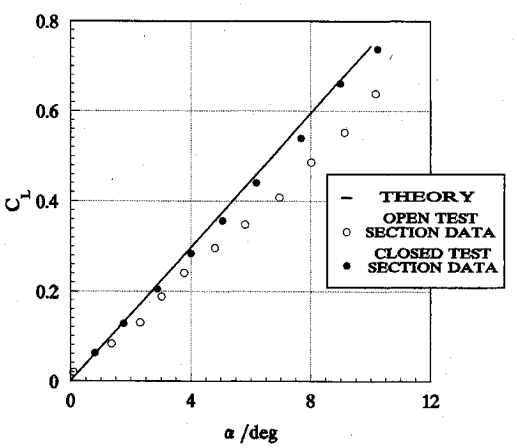

Fig. 5 Lift characteristics of tanker wing.

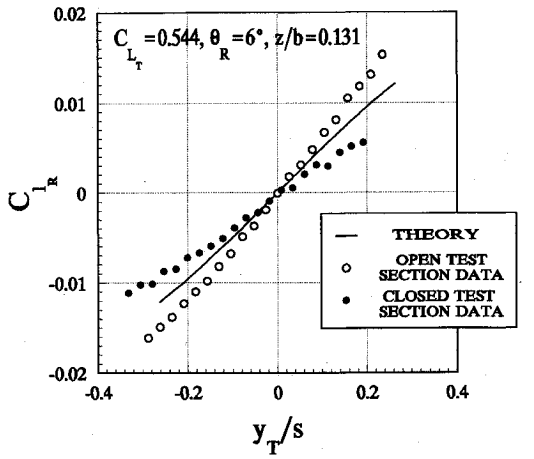

Fig. 6 Receiver aircraft rolling moment coefficient due to sideways displacement of tanker wing.

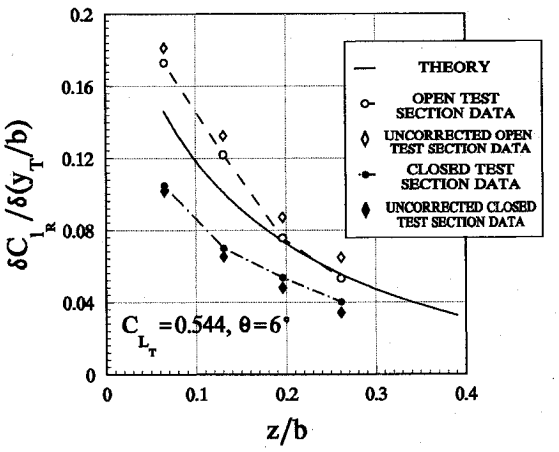

Fig. 7 Variation of receiver aircraft rolling moment due to sideways displacement of tanker wing derivative $\partial C_{l_R}/\partial(y_T/b)$ with vertical separation.

to reduce the relative sideways displacement. Figure 6 also shows the experimental data obtained in the open and closed test sections. The data are presented with the boundary interference correction estimated using the image vortex system described previously. For the closed test section, displacement of the tanker wing to starboard increases the upwash over the receiver starboard wing and reduces the rolling moment derivative $\partial C_{l_R}/\partial(y_T/b)$. The opposite applies to the open test section. Part of the remaining difference between the two sets of corrected data is due to the different vertical positions of the tanker wing vortex wake, which is difficult to estimate since the interference varies considerably across the tanker wing span. In the closed test section the effect of the wall interference is to reduce the downwash from the tanker wing, and therefore, effectively increase the vertical separation between the tanker wing and receiver aircraft. The downwash over the receiver wing and the corresponding rolling moment due to sideways displacement are reduced while the opposite effect is produced in the open test section.

As usual, the theoretical values of the aerodynamic derivatives are determined at the datum position which is with zero sideslip and wings level on the centerline of the tanker wing wake. Figure 7 gives the rolling moment due to sideways displacement derivative data in both corrected and uncorrected form together with the theoretical variation over the range of vertical separation tested. This derivative depends on the rate of change of downwash due to the tanker across the receiver wing span, and higher values occur near the wing tip and at low vertical separation between tanker and receiver. The theory, which includes the relatively small fin contribu-

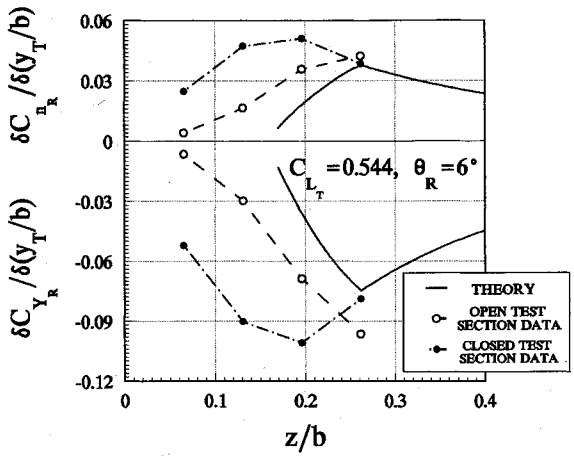

Fig. 8 Variation of aerodynamic derivatives $\partial C_{n_R}/\partial(y_T/b)$ and $\partial C_{Y_R}/\partial(y_T/b)$ with vertical separation.

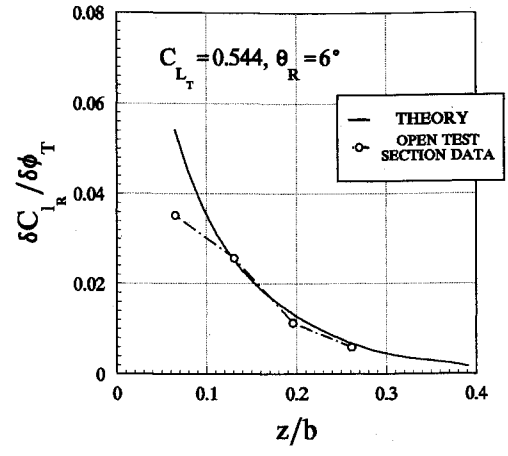

Fig. 9 Variation of receiver aircraft rolling moment due to tanker wing bank derivative $\partial C_{l_R}/\partial\phi_T$ with vertical separation.

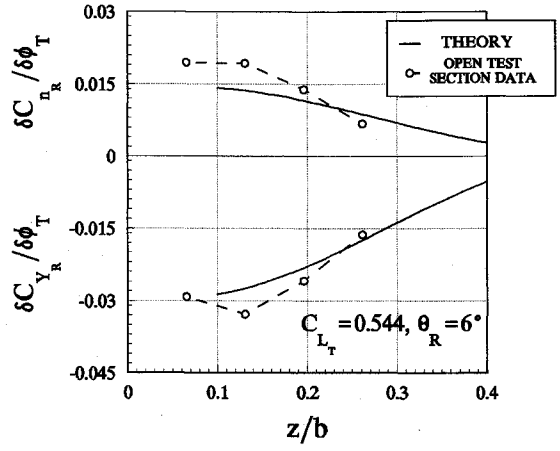

Fig. 10 Variation of aerodynamic derivatives $\partial C_{n_R}/\partial\phi_T$ and $\partial C_{Y_R}/\partial\phi_T$ with vertical separation.

tion, can be seen to lie between the open and closed test section data. The corresponding variation of the side force and yawing moment derivatives, which are due mainly to the effect of sidewash at the fin, are shown in Fig. 8. The yawing moment includes the small contribution from the main wing associated with the variation of induced drag across the span, while the ratio of the side force to yawing moment is approximately equal to the wing span/fin arm which has the value 2. Based on the peak values, the theory underpredicts, although insufficient data were taken with the open test section to determine the peak position accurately. The variation with vertical separation is similar for theory and experiment. The peak value occurs when the tip of the receiver fin intersects the vortex wake of the tanker wing. In theory, this occurs at the vertical separation $z/b = 0.25$ ($z = 19$ cm) allowing for the receiver pitch angle of 6 deg and the vertical displacement of the tanker wake which is approximately 10% of the wing span (=8 cm). The difference in the tanker wake positions in the open and closed test sections also accounts for some of the observed difference in the side force and yawing moment data. At the receiver fin this difference is estimated as $2\frac{1}{4}$ cm ($\delta z/b = 0.03$).

In the case of the bank angle displacement tests, experimental data were obtained only from the open test section by rotating the tanker wing. This rotation produces a sideways displacement of the receiver aircraft relative to the tanker wing wake which is proportional to the vertical separation. The direction of the sideways displacement is such that the measured forces and moments are less than those produced by banking the receiver aircraft. As in the sideways displacement case, the direction of the rolling moment on the receiver aircraft due to the bank displacement acts in the stable sense, tending to reduce the bank displacement. The rolling moment depends on the rate of change of the tanker downwash in the vertical direction which is most sensitive to the roll up of the wake near the wing tip. Figure 9 shows the variation of the rolling moment due to bank derivative with vertical separation between tanker and receiver. The theory compares favorably with the experimental data. The prime contribution to the side force and yawing moment is due to the effect of the component of the tanker wing downwash acting normal to the receiver fin. As the receiver is banked relative to the tanker, a sidewash component equal to the tanker downwash times the bank angle is produced. Therefore, this component is highest at low vertical separation between tanker and receiver. The side force and yawing moment due to bank are shown in derivative form in Fig. 10. Again, the theory compares favorably with the experimental data.

The remaining tests involved yawing the receiver aircraft model with and without the tanker wing in position, and the results are presented in the form of the difference between the values obtained from the tanker and receiver combination and the receiver only. The effect of yaw is to produce sidewash at the receiver fin mainly from the tanker wing vortex wake and partly from the receiver wing. Due to the sidewash from both the tanker and receiver wings, the receiver aircraft is less stable in yaw. Side force and yawing moment due to yaw derivative data and theoretical results are given in Fig. 11. In the case of the yawing moment, the theory indicates a peak reduction in stability slightly less than the experimental value at a vertical separation $z/b = 0.25$ ($z = 19$ cm) which, as discussed in the sideways displacement case, corresponds to the tip of the fin intersecting the tanker wing wake. From experiment, the peak reduction occurs at a similar vertical separation and is in the region of $z/b = 0.23$ ($z = 18$ cm). The reduction represents approximately 14% of the receiver aircraft's directional stability derivative $\partial C_n/\partial\beta$ which is equal to 0.19. Adding a fuselage to the receiver aircraft model would lead to a larger reduction in the aircraft stability. The destabilizing effect of the fuselage is enhanced by the tanker wake and, typically, the overall reduction in aircraft stability would be doubled. Side force data given in Fig. 11 are similar in form to the yawing moment data since the main contribution is due to the fin. The fin moment arm is half the wing span and, hence, the theoretical side force coefficient is twice the yawing moment coefficient which is roughly in agreement with the measured data. The difference between the two sets of experimental data can only be partly explained. At high values of the vertical separation z/b, the difference is as expected, and as explained previously, is due to the difference in the vertical position of the tanker wake. However, this does not explain the much larger difference obtained at low values of z/b.

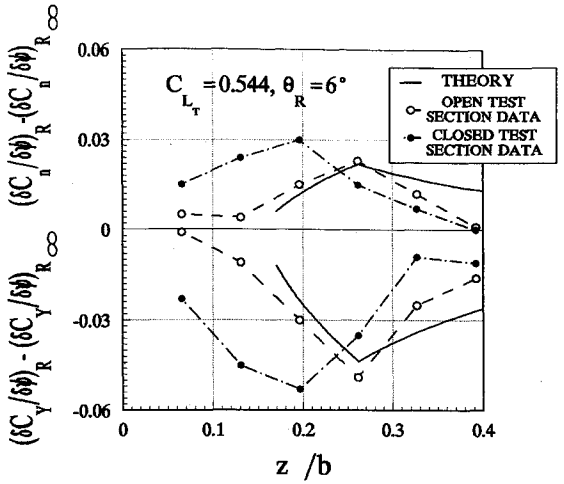

Fig. 11 Variation of yawing moment and side force due to yaw derivatives, $(\partial C_n/\partial\psi)_R$ and $(\partial C_Y/\partial\psi)_R$, with vertical separation.

Some additional tests were made to investigate the effect of the tanker fuselage on the aerodynamic interference between the tanker and receiver in yaw. As previously described, the tanker wing was set low and at incidence of 4 deg on the fuselage. The yaw tests were then repeated. Practically no difference was found between the data obtained from the tanker wing with fuselage and from the tanker wing only.

Conclusions

Predictions from the aerodynamic model of a tapered tanker wing and receiver model have been compared with data obtained in a low-speed wind tunnel. Since the experimental and theoretical variations with sideways, bank, and yaw displacements are essentially linear, the data and theory are presented in derivative form. Due to the relatively large wind-tunnel models, significant wind-tunnel boundary interference effects were found in the experiment. These were assessed by taking measurements in both open and closed test sections.

Two of the most significant derivatives are the rolling moments due to sideways and bank displacements. In the case of the rolling moment due to sideways displacement data, corrections are made using the method of images applied to the tanker and receiver wings in a rectangular test section. Part of the difference between the two sets of corrected data is due to the different vertical positions of the tanker wake in the open and closed test sections. The experimental variations of the derivatives $\partial C_{l_R}/\partial(y_T/b)$ and $\partial C_{l_R}/\partial\phi_T$ with vertical separation are similar to the theory. Unlike previous results obtained using a rectangular untwisted tanker wing, both theory and experiment give significant side force and yawing moment when the receiver fin is displaced from the centerline of the tanker wake. This is due to the sidewash at the fin from both the tanker and receiver wing wakes. When the receiver is displaced in yaw the induced sidewash gives a loss in directional stability of the receiver aircraft. Overall, the theory compares favorably with the experimental data.

Acknowledgments

The authors gratefully acknowledge the continuing support of the Ministry of Defence and the Science and Engineering Research Council through a joint research grant and the assistance of J. Bradley and A. M. Oliver at the Aircraft and Armament Experimental Establishment, Boscombe Down.

References

[1]Bradley, J., "The Handling and Performance Trials Needed to Clear an Aircraft to Act as a Receiver During Air-to-Air Refuelling," AGARD CP 373, Flight Test Techniques, Paper 9, July 1984, pp. 9-1–9-16.

[2]Bloy, A. W., Lamont, P. J., Abu-Assaf, H. A., and Ali, K. A. M., "The Lateral Dynamic Stability and Control of a Large Receiver Aircraft During Air-to-Air Refuelling," *Aeronautical Journal*, Vol. 90, June–July 1986, pp. 237–243.

[3]Bloy, A. W., Ali, K. A. M. and Trochalidis, V., "The Longitudinal Dynamic Stability and Control of a Large Receiver Aircraft During Air-to-Air Refuelling," *Aeronautical Journal*, Vol. 91, Feb. 1987, pp. 64–71.

[4]Bloy, A. W., and Trochalidis, V., "The Performance and Longitudinal Stability and Control of a Large Receiver Aircraft During Air-to-Air Refuelling," *Aeronautical Journal*, Vol. 93, Dec. 1989, pp. 367–378.

[5]Kuchemann, D., "A Simple Method for Calculating the Span and Chordwise Loading on Straight and Swept Wings of Any Given Aspect Ratio at Subsonic Speeds," Royal Aircraft Establishment Aerodynamics Rept. 2476, 1952.

[6]Margason, R. J., and Lamar, J. E., "Vortex-Lattice Fortran Program for Estimating Subsonic Aerodynamic Characteristics of Complex Planforms," NASA TN D-6142, Feb. 1971.

[7]Bloy, A. W., and Trochalidis, V., "The Aerodynamic Interference Between Tanker and Receiver Aircraft During Air-to-Air Refuelling," *Aeronautical Journal*, Vol. 94, May 1990, pp. 165–171.

[8]Bloy, A. W., Trochalidis, V., and West, M. G., "The Aerodynamic Interference Between a Flapped Tanker Aircraft and a Receiver Aircraft During Air-to-Air Refuelling," *Aeronautical Journal*, Vol. 95, Oct. 1991, pp. 274–282.

[9]Grow, T. L., "Effect of a Wing on Its Tip Vortex," *Journal of Aircraft*, Vol. 6, No. 1, 1969, pp. 37–41.

[10]El-Ramly, Z., and Rainbird, W. J., "Flow Survey of the Vortex Wake Behind Wings," *Journal of Aircraft*, Vol. 14, No. 11, 1977, pp. 1102–1108.

[11]Hoganson, E. H., "A Study of Aerodynamic Interference Effects During Aerial Refuelling," M.S. Thesis, Air Force Inst. of Technology, AD-A136895, Wright-Patterson AFB, OH, 1983.

[12]Alford, W. J., "Theoretical and Experimental Investigation of the Subsonic-Flow Fields Beneath Swept and Unswept Wings with Tables of Vortex-Induced Velocities," NACA Rept. 1327, 1957.